International Journal of Engineering

Journal Homepage: www.ije.ir

Experimental and Nonlinear Analysis of Cracking in Concrete Arch Dams Due to Seismic Uplift Pressure Variations

M. J. Kadhim[a], T. J. M. Alfatlawi[a], M. N. Hussein*[a,b]

[a] *Civil Engineering Department, University of Babylon, Babylon, Iraq*
[b] *Civil Engineering Department, Iraq University College, Basrah, Iraq*

PAPER INFO

Paper history:
Received 21 November 2020
Received in revised form 19 March 2021
Accepted 25 March 2021

Keywords:
Arch Dams
Degree of Curvature
Earthquake
Extended Finite Element
Shake Table

ABSTRACT

Cracked concrete arch dam's behavior due to moderate earthquake magnitude and water pressure variation was investigated. Plain concrete was used to cast the dam's models with 45 Mpa design strength. A shake table has been planned, manufactured, and built to create a dynamic testing facility. The experimental work was included testing of four scaled-down concrete arch dams' models, which is divided into two groups, each group contains two different degrees of curvature models. An artificial crack was made at the center of the dam's body. The extended finite element method (XFEM) is outlined in order to address the numerical predicate for the propagation of a crack. The results showed a good behavior of all arch dams under moderate earthquake intensity. The arch dam with a higher degree of curvature recorded 17.8% and 16.2% lower displacement at Z and X-direction, respectively. The stress evaluation and crack propagation in comparison with the arch dam owns the lowest degree of curvature. Hence, increasing the degree of curvature led to raising the stability of the dam, earthquake resistance, less displacement, and less growth of tensile cracks.

***doi**: 10.5829/ije.2021.34.05b.09*

1. INTRODUCTION

A dam is a hydraulic structure of nearly impermeable material created over a river to create a reservoir on its upstream side to impound water for different purposes. This may include drainage, water management, flood control, navigation, agriculture, tourism, and the most important purpose is hydropower. At first, dams were initially designed by humans to deal with the needs of small settlements for agriculture [1, 2]. Dams have begun to be used not only for irrigation but for water storage and hydroelectric power [3] depending on the location of the dam. Hydropower produces 19% of the world 's overall energy supply and is widely used in more than 150 countries and water-rich countries like Canada, Norway and Brazil that almost solely use dams for hydropower output [4].

Dams can be classified according to construction design [5] or the structures used to endure tension due to water pressure [6] in the reservoir into two types as gravity and arch dams. The most popular type of concrete dam is a concrete gravity dam that is shown in Figure 1. In this type of dam, the concrete and friction mass weight resist the water pressure of the reservoir and is made of non-reinforced vertical concrete blocks with flexible seals in the joints between the blocks. In cross-section, concrete arch dams are usually very small, as shown in Figure 2. The water forces of the reservoir acting on an arch dam are brought onto the abutments laterally, formed from a series of thin vertical blocks connected together, with water stopping between the blocks [7, 8].

Arch dams are subjected to assortment types of loads, most of the time it is static caused by water pressure, dam's self-weight, temperature variation [9, 10], and ice loads. In some cases, subjected to dynamic loads such as traffic loads, wind loads and seismic loads which is the most dangerous case. The seismic loads can play an important role in its effect to the arch dams especially if

*Corresponding Author Institutional Email: *mohammed.alhashimi@iuc.edu.iq* (M. N. Hussein)

Please cite this article as: M. J. Kadhim, T. J. M. Alfatlawi, M. N. Hussein, Experimental and Nonlinear Analysis of Cracking in Concrete Arch Dams Due to Seismic Uplift Pressure Variations, International Journal of Engineering, B: Applications Vol. 34, No. 05, (2021) 1156-1166

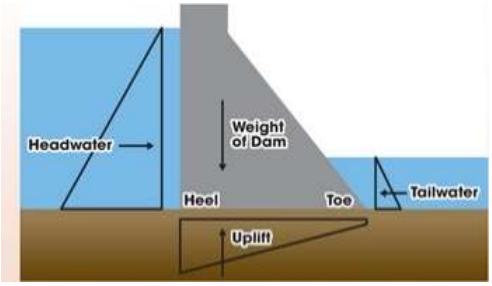

Figure 1. Concrete gravity dam

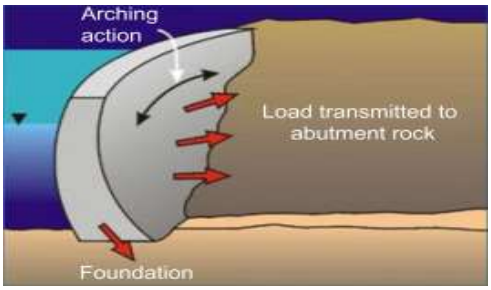

Figure 2. Concrete arch dam

these dams are subjected to prior deformations, such as cracks. The importance of studying the risk of seismic loads on arched dams lies in the extent of their impact on the stability of the dam and the response of the dam to it, which preserves its structure and prevents the development of cracks on it.

A variety of earthquake research studies on concrete arch dams have previously stated that complex impacts on arch dams should be taken into account in the ground motions. It also presents an arch dam's three-dimensional linear earthquake response. In the finite element analysis, various soil motion results are taken into account and, in addition to rigid and elastic base conditions [11].

Researchers have recently studied the impact of earthquakes on concrete arch dams and found that most of the modern dams in regions exposed to seismic activities have been built utilizing techniques that are now becoming simplistic and unreliable. The damage sustained by the few dams that have been exposed to extreme ground movements, such as Hsinfengkiang Dam in China, the Pacoima Dam in the U.S. and Koyna Dam in India, along with the increasing concern about the earthquake protection of sensitive infrastructure, has driven substantial interest in modern study and exploration of existing dams. The seismic protection of several dams has been tested over the past 20 years, and some of them have been improved to enhance their seismic tolerance [12, 13].

Concrete failure is a crack forming and development process [14]. In recent years, there has been an increasing interest in the study of the relationship between seismic effects and cracks developed in arch dams. One of the main obstacles is the process of representing the arch dam and conducting practical experiments on it, which requires equipment and high costs. The main objectives of this paper can be listed as follows;

- Make an experimental investigation to examine the behavior of arch dam under seismic loads and uplift pressure variations.
- Investigate the propagation of crack of the arch dam under seismic loads and uplift pressure variations.
- Use the extended finite element method (XFEM) for analysis of the arch dams and to predict the crack propagation and the development of other cracks under water pressure and seismic loads.

2. ARCH DAM CLASSIFICATION

Arch dams are classified according to the ratio of their thickness to their height into three sections:

1. Thin if $(\frac{b}{h}) \leq 0.2$.
2. Medium-thick $(\frac{b}{h})$ = (0.2-0.4).
3. Thick $(\frac{b}{h}) \geq 0.4$.

According to the new classification if $(\frac{b}{h}) > 0.65$. then there will be a fourth type called (Arch gravity dam). Also, arch dams are classified according to their height as :

1. Low arch dam if h ≤ 30m
2. Medium if h = (31m - 90m)
3. Large if h ≥ 91m.

Only thin arch dams need reinforcement which is not needed for other forms of dams because it greatly raises the cost [15–19].

3. SHAKING TABLE DESIGN

A uniaxial shake table with a rotating platform capability (2DOF; axial and rotational degrees of freedom) was planned, manufactured and built to create a dynamic testing facility, which is servo-electrically controlled and powered by low-friction ball bushing bearings. To ensure an effective reproduction of input motion by the shake table method, a system has been assembled with caution. In the time and frequency domain, arbitrary comparisons of input signal verses shake-table response have been used to calculate the simulator's abilities to replicate earthquake movements scaled according to similarity rules.

The electrical shake table is shown in Figure 3. It was completely manufactured locally under the direct supervision of the researcher and his supervisors uniaxially with an ability of a rotating platform in two horizontal directions.

Figure 3. Shaking table developed as experimental rig

4. EXPERIMENTAL PROGRAM

4. 1. Dimension Analysis A dimensional analysis was conducted with the aid of Buckingham (π) theorem to establish similarity relationships between systems [20, 21]. Scale factors obtained by dimensional analysis is reflected in the relation between prototype and model. The real dam that was chosen for the purpose of taking on the climatic conditions and the real loads that it is exposed to, and applied to the proposed models for the purpose of conducting the present study on the Dinas Arch Dam located in Wales City in the UK [22] with 14m height. The similitude necessities for dynamic relationships between the model and prototype rely on the geometric, material properties of the structure and on the sort of force applied to the structure. Whether we need to obtain dynamic similitude we should have geometric similarity jointly with kinematic and dynamic similarities [23, 24]. Because of the calamitous nature of earthquakes, this kind of force wants to be taken industriously into consideration in the design of structures. Replica models for shake table testing ought to satisfy both the Froude and Cauchy scaling requirements as aforesaid in Equations (1) and (2), respectively; which implies the simultaneous replication of inertia, restoring and gravitational forces [25].

$$Fr = \frac{V^2}{l.g} \quad (1)$$

$$Ca = \frac{\rho.v^2}{E} \quad (2)$$

Since the value of gravitational acceleration (g) must be equal to one, and from the dimensional analysis we get the dimensionless product of Sa/Sg =1 (a is the imposed acceleration), the following scaling law is derived:

$$SE/\rho = SL \quad (3)$$

This is hard to understand because it requires that the model material has a massive mass density or small modulus or even both. A better alternative is to raise the density [15], of the structure with extra non-structural material. Similitude requirements for earthquake modelling is detailed in Table 1. Geometric dimensions of the model were obtained by directly scaling the prototype dimensions by the scale factor S_L = 15.6.

TABLE 1. Similitude requirements for earthquake modelling [21]

Parameter	Dimension	Scale Factor
Modulus E	FL^{-2}	S_E
Force Q	F	$S_E S_L^2$
Pressure q	FL^{-2}	S_E
Linear Dimensions	L	S_L
Density ρ	$FL^{-4}T^2$	$\frac{S_E}{S_L}$
Time t	T	$S_L^{0.5}$
Frequency ω	T^{-1}	$S_L^{0.5}$
Gravity Acceleration G	LT^{-2}	1

4. 2. Criteria for Arch Dam and Material Properties Such structures are designed primarily to carry only gravity, uplift pressure, and hydrostatic loads. Therefore, seismic resistance is not regarded. In this study, a single curvature scaled-down arch dams were simulated with two different curvatures to assess stress distribution over the dam, displacement of the concrete arch dam, and follow-up to the spread of crack underwater pressure and intensity of the earthquake. The dams in this investigation are depending on optional information brought by Manual-EM 1110-2-2201 [18]. However, the model used in this study is a typical model and the crack is created artificially to the model to assess the crack propagation at the center of the dam. The site, water reservoir information, the weather, and other significant details for dam plan and design were given. Typical values have been chosen to understand the properties of the materials. Experimentally, two solid 3D plain concrete medium-thick arch dam models with two different curvatures (1 model for each curvature) used in this study are shown in Figures 4 and 5; fixed from the bottom with dimensions and properties as the detail is summarized in Table 2. An artificial crack made at the center back of the dam's body is shown in Figures 6 and 7 with its dimensions as 200 mm length, 20 mm height, and 20 mm depth.

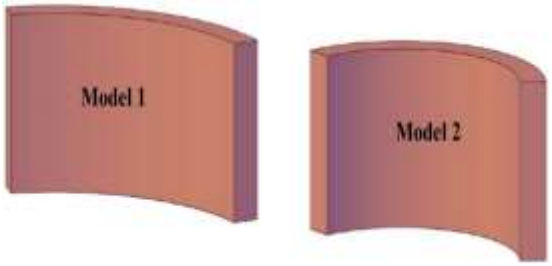

Figure 4. Arch dam models

Figure 5. Concrete arch dam models

Figure 7. Concrete arch dam with artificial crack

TABLE 2. Dimensions and properties

Dimensions		
Dimension	**Model 1**	**Model 2**
Outer length (mm)	1700	1700
Inner length (mm)	1500	1380
Radius (mm)	1188	650
Height (mm)	900	900
Thickness (mm)	180	180
°: Degree of curvature, L/r = 0.017° [26]	74°	124°
Materials Properties		
Property	**Model 1**	**Model 1**
Compressive strength, f_{cc}	44.45 Mpa	44.55 Mpa
Density of Concrete	2400 (Kg/m^3)	2400 (Kg/m^3)
Poison's ratio	0.2	0.2
Modulus of elasticity, E_c = 4700 $\sqrt{f_{cc}}$ [27]	31370 (Mpa)	31370(Mpa)
Fracture Energy, G_F = 1041 (1- $e^{-0.07 f_{cc}}$) [28]	951.2 (N/m)	951.2 (N/m)

4. 3. Experimental Tests The model is installed as shown in Figure 8 with fixed the bottom by concrete. The shake table operated to apply a two-dimensional earthquake intensity. Moderate magnitude (5.7M) of actual earthquake records are selected from the Pacific Earthquake Engineering Research Center (PEER) ground motion database [29–31]. The acceleration of (Mammoth Lakes-04) earthquake is presented in Figure 9. A water pressure was applied to the surface of the crack using a pressure compressor with a capacity of 10 bars, as shown in Figure 10a. A 5% ratio of damping in the system of damping was considered. Up to the full reservoirs, the water level is assumed to be 14 m. A combination of multiple loads will be applied to the dam models consisting of static loads (water pressure + dam's self-weight) and dynamic loads (earthquake + hydrodynamics). Due to dam's gravity, the static solutions of the dam weight and hydrostatic loads in the initial situations are taken as the system's diverse evaluations. The Westergaard's [32, 33] virtual mass is employed to provide the influence of hydrodynamics. The importance of the simulated mass of Westergaard [34] is M_i^1 at node *i* on the upstream of the dam's surface is:

$$M_i^1 = \frac{7}{8}\,\rho_w \frac{b_{i1}+b_{i2}}{2}\sqrt{hy_i} \quad (4)$$

where (h) refers to the water's depth, (ρ_w) refers to the mass density of water, (y_i) represents the distance between the surface of the water and node (i), and (b_{i1}) and (b_{i2}) refer to the lengths of the edges of quadrilateral constant-strain elements next to node (i) on the dam's upstream surface. It is worth emphasizing that the analysis does not include consideration of seismic water pressure effects within the cracks. It is important to investigate in greater depth the impact of seismic water pressure on crack propagation, as well as the dam's dynamic response.

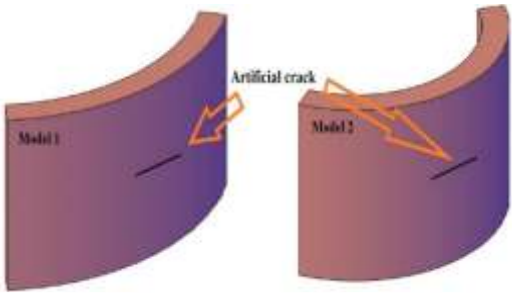

Figure 6. Arch dam model with artificial crack

Figure 8. Concrete arch dam model with fixed support

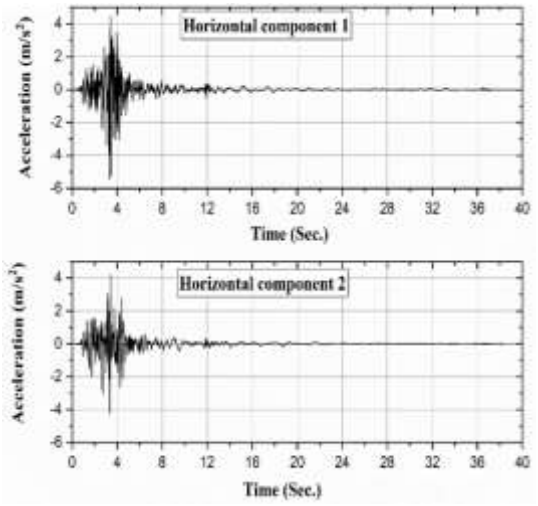

Figure 9. Acceleration components

Figure 10. (a: applied water pressure, b: measurement of displacements. c: concrete strain gauge)

Linear displacement sonic transducers were used to measure the absolute response displacements in the longitudinal (horizontal) direction during the shaking table tests fixed as shown in Figure 10b. The LVDT fixed at coordinates mesured from the center of the dam as (0,-0.15,0) for LVDT in Z-direction and (-0.75,-0.15,-0.5) for LVDT in X-direction and (-0.75,-0.15,-0.5) in Y-direction? The displacement transducer has a stroke of ±100 mm. There is a variety of mechanical and electrical methods of measuring strain, but owing to their superior measurement properties, the vast majority of stress measurements are conducted using strain gauges. Form (PL-60-11-3LJC-F) concrete strain gauges were used in the experimental method, with the following characteristics: wire form, with the stiffness of 119±0.5 percent, a gauge factor of 2.08±1 percent, a gauge length of 60 mm, and a gauge width of 2.5 mm with a maximum strain of 2 percent as shown in Figure 10c.

4. 4. Selection of the Ground (Shaking Table) Excitation Ground Motion for the Accelerogram Portion of Mammoth Lakes-04 (Figure 9) was implemented at a moderate amplitude to determine the output of the model structure under seismic excitation. The initial accelerogram has a complete duration of 40 seconds of the ground excitation period with peak acceleration 4.4 $\frac{m}{s^2}$. To satisfy the criteria for consistency, the used record was time-compressed by a factor of $S_T = \sqrt{S_L}$. While, there were around 10.3 seconds of active seismic excitation time after time compression as shown in Figure 11.

5. NONLINEAR ANALYSIS

As part of the research, the same concrete arch dam models are established and the numerical solutions are correlated with the experimental results. The models are created and analyzed by using the (XFEM) method. A strong and robust process program is compulsory for the analysis. ABAQUS/CAE 6.13 (2017) software was used to specify the nonlinear dynamic analysis in this study. The numerical models have the same geometry, dimensions, and boundary conditions of the prototype of the tested arch dam models.

5. 1. Dam Modeling by XFEM Belytschko and Black's [35] extended finite element technique encompasses substantial advantages in relation to crack propagation numerical modeling. Moreover, this method does not require the finite element mesh to correspond to the presence of cracks. Likewise, there is no requirement for the remeshing for crack growth. This is a consequence of the displacement vector function approximation which is appended to model the crack's existence. When the crack is modelled using XFEM, the classical displacement is predicated on the finite element approximation in conjunction with the partition of unity method (PUM) paradigm, as per Melenk and Babuška [10, 36, 37]. This permits easy incorporation of local

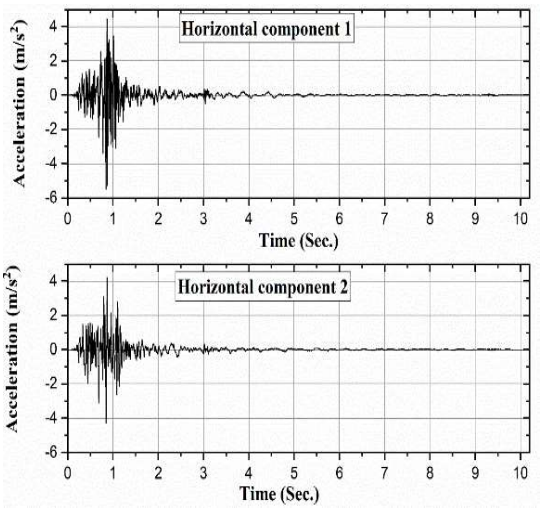

Figure 11. Scaled Down Mammoth Lakes-04 Components

enrichment functions into the finite element approximation. Specifically, enrichment functions generally comprise near-tip asymptotic functions which apprehend the uniqueness encircling the crack tip and an intermittent function that signifies the displacement leap across the surfaces of cracks. Currently, the XFEM method is employed to represent the crack initiation and proliferation manifest in concrete gravidynamics, as per ABAQUS/CAE for brittle or ductile materials, such as the concrete gravity dams modeled in the current work [38, 39]. This process is described in more detail in the ensuing sections of this paper.

The (XFEM) emerged from the cohesive segments method [40, 41]. When it is employed in unison with the phantom node technique [42–44], it is possible to replicate crack initiation and proliferation in an indiscriminate direction. This is because the crack propagation is not bound to mesh-based element peripheries. The crack tip position does not need to be specified with this method. Rather, it is only necessary to indicate a region of reference in which the crack will proliferate. Furthermore, no near-tip asymptotic singularity is required. It is merely necessary to contemplate the displacement jump across a cracked element. This means that the crack is obliged to proliferate across a complete element in an instant in order to obviate the necessity of modelling stress singularity. The phantom node approach superimposes the phantom elements, rather than incorporating further elements of freedom. In this way, this method is able to describe discontinuity and can be readily encompassed within traditional finite element codes. XFEM can be employed in relation to 2D [38, 42, 45, 46], 3D problems [45, 47–49], and dynamic problems [50–52].

5. 2. Three Dimensional Modeling and Mesh Distribution In order to model the concrete members, a 3D first order diminutive integration continuum elements (C3D8R-Brick) are applied. These components are flexible and can be used in models for basic linear analysis or for complex nonlinear interaction [53, 54], plasticity, and large deformation analyses. A normal concrete discretization mesh is presented in Figure 12.

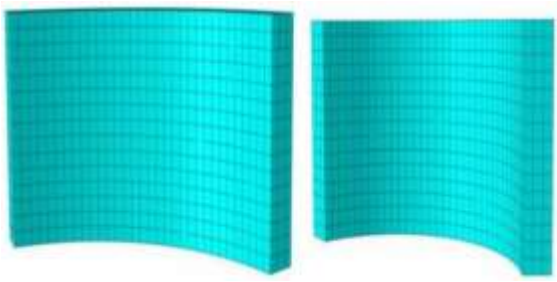

Figure 12. Concrete members discretized using brick elements

5. 3. The Model Calibration and Evaluation It cannot describe how the content changes due to damage by determining damage initiation. The damage is modelled within ABAQUS employing a scalar damage criterion (D) .This can vary from 0 which means (no - damage) to 1 which means (complete - failure). To measure the stress, including damage, the stress that would have been there without damage is multiplied by $(1-D)$. This contributes to the undamaged reaction without damage $(D=0)$, the stress is 0 with complete failure $(D=1)$ and persists in between a fraction of the stress (see Figure 13) [39, 55].

It is important to determine either the maximum displacement or the fracturing energy that is the field under the curve in traction versus the separation graph. The softening behavior can be defined by various options: how the traction-separation graph goes from the point at the beginning of damage to the fully failed state. In this case, linear softening is used, which in the traction-separation graph refers to a straight line. Mode mixing may be taken into consideration, with the BK law, power-law, or tabular data defined. Alternatively, it is possible to indicate model-independent behavior. Owing to the softening of the material model, simulations like damage evolution frequently lead to convergence difficulties. ABAQUS facilitates the use of viscous regularization during damage to stabilize the reaction. The tangent stiffness matrix will then be positive definite for sufficiently small-time measures. As a sub-option for Maxps impact, a viscosity coefficient may be defined. It should be selected in such a way that the effect on the final outcome of the stabilization is negligible. The ALLVD (viscous dissipation) production can be compared to ALLSE (strain energy) to verify this. In contrast with ALLSE, if ALLVD is not thin, viscous stabilization is likely to affect outcomes. Playing around with the coefficient of viscosity will help produce a fair outcome in a reasonable period of time [39, 55]. Apart

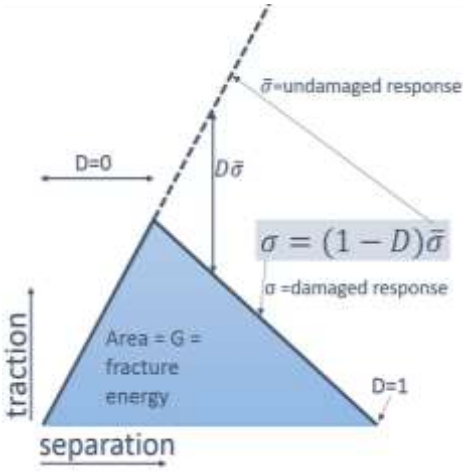

Figure 13. Damage evaluation

from determining when the material will be damaged and how it will respond after the damage is started, it is important to define the area where a crack can occur. This is the area where the words for enrichment can be applied. To permit the crack to spread, the 'allow crack growth' box should be checked. XFEM may also be used for stationary splits, which enables the measurement of contour integrals with less meshing effort. It is possible to insert a different component reflecting the crack (without property or mesh) into the assembly and move it to the correct location. The crack is described by selecting this portion as a crack position. The crack does not have to be around the edges of the part. In fact, if the crack crosses through the part, the XFEM method functions better. For interaction between both sides of the crack, frictionless small-sliding interaction can be described. The solution controls can be changed to help in achieving a converged solution. It is possible to verify discontinuous analysis in the time incrementation column. This makes it possible for ABAQUS to do further iterations before seeing whether the answer goes somewhere. The parameter (I−A) can be increased from the default (5) in the first More tab, to make ABAQUS more attempts before the simulation is aborted. Increasing the number of attempts is helpful if major cut-backs are needed. ABAQUS immediately produces an iso-surface view cut based on this performance if PHILSM is required, which displays the position of the break. The crack will not be noticeable when it is not requested, and the effects displayed will be counterintuitive. STATUxSXFEM is also XFEM-specific. It gives the position of the enriched elements, if the element is undamaged it is (0.0), if the element is absolutely cut through (no traction forces exist), and if the element is weakened but certain traction forces exist, it is a value in between. Of course, natural outputs are also available, such as stress and pressure.

6. EXPERIMIANTAL RESULTS

Two model arch dams were tested using the time-compressed Mammoth Lakes-04 1980 earthquake in two horizontal directions of excitations. one model (M1) with 74˚ degree of curvature and one model (M2) with 124˚ degree of curvature. Traces of the dam displacement, stresses, crack propagation, and table motion was recorded during each test. The test program was thus selected so that the models were exposed to 14 m maximum reservoir water level. The time-history of the dam displacements, stress distribution (see Figure 14), and crack propagation during Mammoth Lakes-04 are extracted from the experimental test as will present in this section.

6. 1. Time History Results during Moderate Seismic Excitation with Water Pressure During the moderate magnitude, both models show a good response to the applied ground motion excitation without any damage evaluation. The results, as shown in Figures 15 and 16, indicate that M2 provides a good response

Figure 14. Strain gauges fixed in three points all over the model to verify the stress development during the test

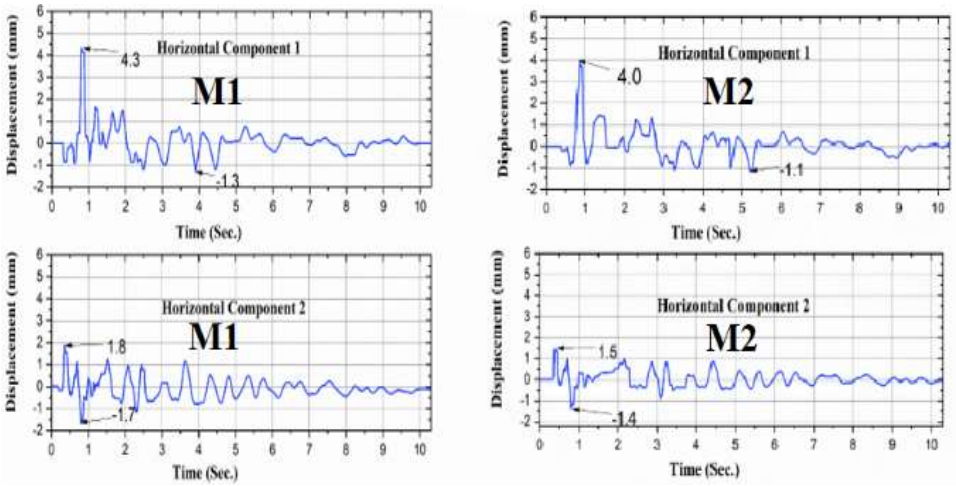

Figure 15. The response of M1 and M2 in Z, X direction, moderate magnitude 5.7M

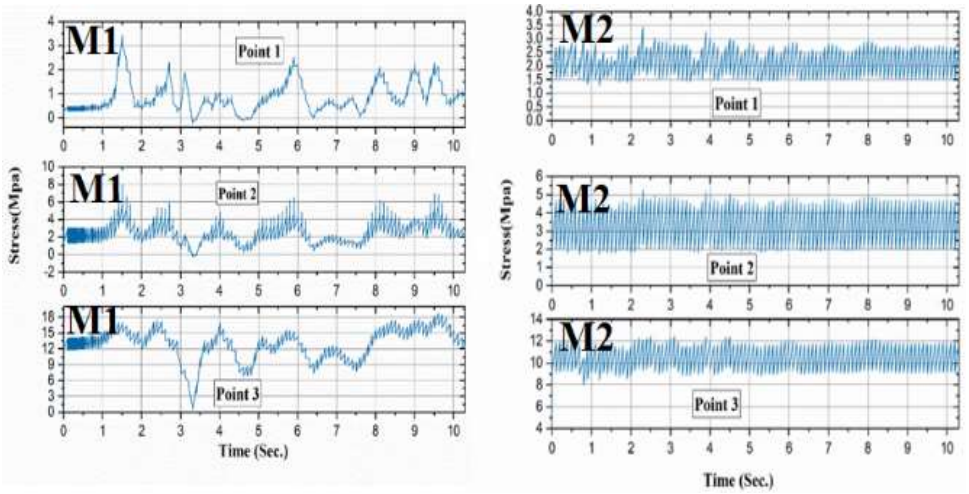

Figure 16. The-maximum principal stresses occurred in points 1, 2 and 3 for M1 and M2, moderate magnitude

compared to M1. The horizontal component 1 (Z-Direction) records the max displacement response compared to the horizontal component 2 (X-Direction) for models M1 and M2 while the max stress recorded during the test was observed at point 3 near the dam's support. Model M1 shows a slight crack propagation while there is no crack propagation is observed for M2 as shown in Figure 17.

7. NUMERICAL TIME HISTORY OF THE DAMS DURING MODERATE MAGNITUDE WITH WATER PRESSURE

The time-history of the dam displacements, stress distribution, and crack propagation during Mammoth Lakes-04 moderate excitation is presented. Figures 18 to 20 provide an overview of the analytical and experimental results, indicating a satisfactory level of agreement between the two sets of results. Numerical and experiment analysis showed a slight crack propagation in model M1. For model M2, no damages were observed during run Mammoth Lakes-04 5.7M.

Figure 17. Deformation and crack propagation patterns for (M1&M2)

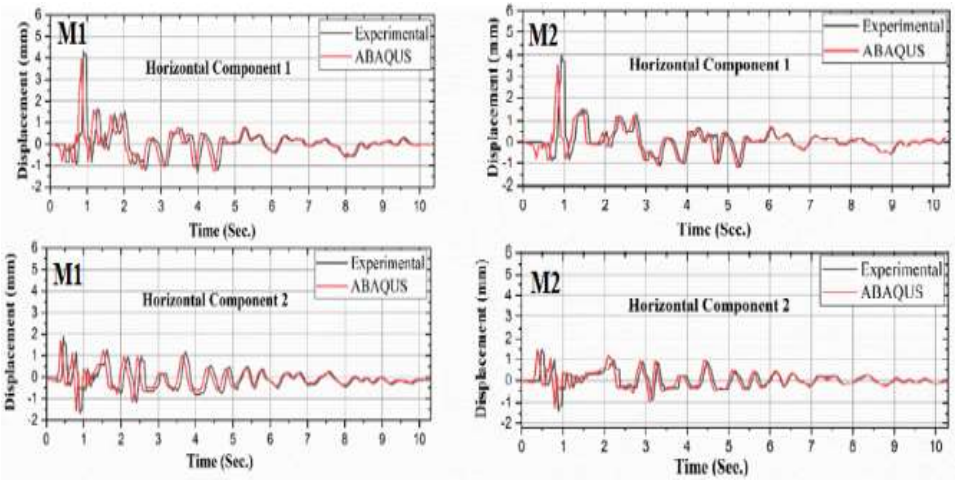

Figure 18. Displacement-time response in horizontal directions of M1and M2 model

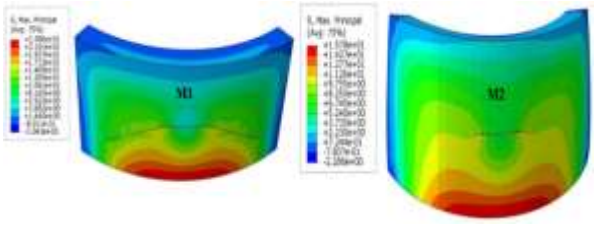

Figure 19. Stress distribution, (S in Mpa)

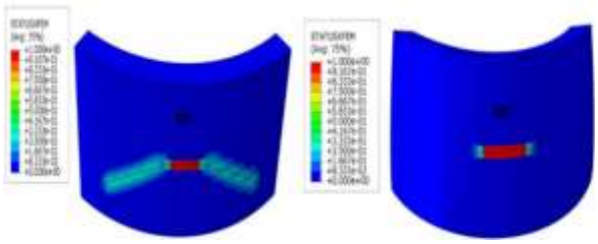

Figure 20. Plastic deformation (STATUSXFE is unitless 0 non-cracked to 1 fully cracked.)

With successive increases in earthquake time until reach to 10.3 second, in model 1, a crack at the middle has propagated from the center into the left and right sides and the max stresses distributed all over the body. Interestingly, model 2 was observed less affected by an increase in earthquake time.

8. CONCLUSION

In the current study, the conclusion can summarize as follow:

1. The curved shape of the dam provides the dam the capability to accommodate the applied loads and increase its stability.
2. For moderate earthquakes, the arch dams may withstand the earthquake even if it contains initial cracks.
3. Non-seismically reinforcement details in medium concrete arch dams do not form a potential source of damage.
4. Most of the deformation and damage development occurred due to the existence of an initial crack.
5. As a method that relies on generalized FEM and the partition of unity method, XFEM is effective for the analysis of discontinuous crack growth in a way that does not rely on the internal geometry and physical interfaces. Consequently, meshing and re-meshing complexities associated with discontinuous problems can be addressed.
6. The degree of curvature is related to the dam's stability. Increasing the degree of curvature make the dam more stable, more responsive to ground motion, less displacement, and less tensile crack development.

9. REFERENCES

1. Marche, C., and Robert, B., "Dam Failure Risk: Its Definition and Impact on Safety Assessment of Dam Structures", ***Journal of Decision Systems***, Vol. 11, Nos. 3–4, (2002), 513–534. doi:10.3166/jds.11.513-534
2. Hartford, D. N. D., and Baecher, G. B., Risk and Uncertainty in Dam Safety, (2004) Thomas Telford Publishing. doi:10.1680/rauids.32705
3. Patsialis, T., Kougias, I., Kazakis, N., Theodossiou, N., and Droege, P., "Supporting Renewables' Penetration in Remote Areas through the Transformation of Non-Powered Dams", ***Energies***, Vol. 9, No. 12, (2016), 1–14. doi:10.3390/en9121054
4. Jabbar Mizhir Alfatlawi, T., Jawad Kadhim, M., and Noori Hussein, M., "Relation between cracks behavior and curvature in cracked concrete arch dam under earthquake", ***Materials Today: Proceedings***, (In Press), (2021). doi:10.1016/j.matpr.2021.02.248
5. Chen, Q., Zou, Y. H., Tang, M., and He, C. R., "Modelling the construction of a high embankment dam", ***KSCE Journal of Civil Engineering***, Vol. 18, No. 1, (2014), 93–102. doi:10.1007/s12205-014-0180-4
6. McManamay, R. A., Oigbokie, C. O., Kao, S.-C., and Bevelhimer, M. S., "Classification of US Hydropower Dams by their Modes of Operation", ***River Research and Applications***, Vol. 32, No. 7, (2016), 1450–1468. doi:10.1002/rra.3004
7. Lin, P., Guan, J., Peng, H., and Shi, J., "Horizontal cracking and crack repair analysis of a super high arch dam based on fracture toughness", ***Engineering Failure Analysis***, Vol. 97, (2019), 72–90. doi:10.1016/j.engfailanal.2019.01.036
8. Javanmard, M., Amiri, F., and Safavi, S., "Instrumentation Readings versus Numerical Analysis of Taham Dam", ***International Journal of Engineering, Transaction A: Basics***, Vol. 32, No. 1, (2019), 28–35. doi:10.5829/ije.2019.32.01a.04
9. Malm, R., Hellgren, R., and Enzell, J., "Lessons Learned Regarding Cracking of a Concrete Arch Dam Due to Seasonal Temperature Variations", ***Infrastructures***, Vol. 5, No. 2, (2020), 1–18. doi:10.3390/infrastructures5020019
10. Mohammadi, M., Samani, H., and Monadi, M., "Optimal Design and Benefit/Cost Analysis of Reservoir Dams by Genetic Algorithms Case Study: Sonateh Dam, Kordistan Province, Iran", ***International Journal of Engineering, Transaction A: Basics***, Vol. 29, No. 4, (2016), 482–489. doi:10.5829/idosi.ije.2016.29.04a.06
11. Karabulut, M., Kartal, M. E., Capar, O. F., and Cavusli, M., "Earthquake analysis of concrete arch dams considering elastic foundation effects", ***Disaster Science and Engineering***, Vol. 2, No. 2, (2016), 46–52
12. Alves, S. W., and Hall, J. F., "Generation of spatially nonuniform ground motion for nonlinear analysis of a concrete arch dam", ***Earthquake Engineering & Structural Dynamics***, Vol. 35, No. 11, (2006), 1339–1357. doi:10.1002/eqe.576
13. Chopra, A. K., "Earthquake Analysis of Arch Dams: Factors to Be Considered", ***Journal of Structural Engineering***, Vol. 138, No. 2, (2012), 205–214. doi:10.1061/(ASCE)ST.1943-541X.0000431
14. Atici, U., Ersoy, A., and Ozturk, B., "Application of destruction specific energy for characterisation of concrete paving blocks", ***Magazine of Concrete Research***, Vol. 61, No. 3, (2009), 193–199. doi:10.1680/macr.2007.00113
15. Boggs, H. L., Tarbox, G. S., and Jansen, R. B., "Arch Dam Design and Analysis", ***Advanced Dam Engineering for Design, Construction, and Rehabilitation***, (1988), 493–539. doi:10.1007/978-1-4613-0857-7_17

16. Xu, Q., Zhang, T., Chen, J., Li, J., and Li, C., "The influence of reinforcement strengthening on seismic response and index correlation for high arch dams by endurance time analysis method", ***Structures***, Vol. 32, (2021), 355–379. doi:10.1016/j.istruc.2021.03.007
17. Jonker, M., and Espandar, R., "Evaluation of Existing Arch Dam Design Criteria in Lieu of ANCOLD Guidelines", ANCOLD 2008 Conference, Australia, (2014), 1–15.
18. US Army Corps of Engineers, ENGINEER MANUAL, No. 1110-2-2200Engineering and Design: Gravity Dam Design, (1995)
19. Ghafoori, Y., Design and Static Analysis of Arch Dam Using Software SAP2000, Master Thesis No.: 33/II.GR, University of Ljubljana, Slovenia, (2016).
20. Shokrieh, M. M., and Askari, A., "Similitude Study of Impacted Composite Laminates under Buckling Loading", ***Journal of Engineering Mechanics***, Vol. 139, No. 10, (2013), 1334–1340. doi:10.1061/(ASCE)EM.1943-7889.0000560
21. Altunisik, A. C., Kalkan, E., and Basaga, H. B., "Structural behavior of arch dams considering experimentally validated prototype model using similitude and scaling laws", ***Computers and Concrete***, Vol. 22, No. 1, (2018), 101–116. doi:https://doi.org/10.12989/cac.2018.22.1.101
22. Federal Energy Regulatory Commission, Engineering guidelines for the evaluation of hydropower projects. Chapter 11-Arch Dams. Washington DC, 20426, (1999), 11–18.
23. Kenan, H., and Azeloğlu, O., "Design of scaled down model of a tower crane mast by using similitude theory", ***Engineering Structures***, Vol. 220, (2020), 110985. doi:10.1016/j.engstruct.2020.110985
24. Xie, W., and Sun, L., "Experimental and numerical verification on effects of inelastic tower links on transverse seismic response of tower of bridge full model", ***Engineering Structures***, Vol. 182, (2019), 344–362. doi:10.1016/j.engstruct.2018.12.046
25. Harris, H., "Use of Structural Models as an Alternative to Full-Scale Testing", Full-Scale Load Testing of Structures, ASTM International, (2009) 25–44. doi:10.1520/STP27137S
26. Kutz, M., Handbook of Transportation Engineering, Vol. 768, McGraw-Hill New York, NY, USA, (2004).
27. Burhan, L., Ghafor, K., and Mohammed, A., "Quantification the effect of microsand on the compressive, tensile, flexural strengths, and modulus of elasticity of normal strength concrete", ***Geomechanics and Geoengineering***, (2019), 1–19. doi:10.1080/17486025.2019.1680884
28. Jin, A.-Y., Pan, J.-W., Wang, J.-T., and Du, X.-L., "A spectrum-based earthquake record truncation method for nonlinear dynamic analysis of arch dams", ***Soil Dynamics and Earthquake Engineering***, Vol. 132, (2020), 106104. doi:10.1016/j.soildyn.2020.106104
29. CAPEER (Pacific Earthquake Engineering Research Center), PEER Ground Motion Database, Pacific Earthquake Engineering Research Center, University of California, Berkeley, US, (2010).
30. Rezaee Manesh, M., and Saffari, H., "Empirical equations for the prediction of the bracketed and uniform duration of earthquake ground motion using the Iran database", ***Soil Dynamics and Earthquake Engineering***, Vol. 137, (2020), 106306. doi:10.1016/j.soildyn.2020.106306
31. Biswas, R., "Evaluating Seismic Effects on a Water Supply Network and Quantifying Post-Earthquake Recovery", ***International Journal of Engineering, Transaction B: Applications***, Vol. 32, No. 5, (2019), 654–660. doi:10.5829/ije.2019.32.05b.05
32. Wang, P., Zhao, M., Du, X., and Cheng, X., "A finite element solution of earthquake-induced hydrodynamic forces and wave forces on multiple circular cylinders", ***Ocean Engineering***, Vol. 189, (2019), 106336. doi:10.1016/j.oceaneng.2019.106336
33. Shahmardani, M., Mirzapour, J., and Tariverdilo, S., "Dynamic Response of Submerged Vertical Cylinder with Lumped Mass under Seismic Excitation", ***International Journal of Engineering, Transaction A: Basics***, Vol. 27, No. 10, (2014), 1547–1556. doi:10.5829/idosi.ije.2014.27.10a.08
34. Wang, M., Chen, J., Wu, L., and Song, B., "Hydrodynamic Pressure on Gravity Dams with Different Heights and the Westergaard Correction Formula", ***International Journal of Geomechanics***, Vol. 18, No. 10, (2018), 04018134. doi:10.1061/(ASCE)GM.1943-5622.0001257
35. Belytschko, T., and Black, T., "Elastic crack growth in finite elements with minimal remeshing", ***International Journal for Numerical Methods in Engineering***, Vol. 45, No. 5, (1999), 601–620. doi:10.1002/(SICI)1097-0207(19990620)45:5<601::AID-NME598>3.0.CO;2-S
36. Geelen, R., Plews, J., Tupek, M., and Dolbow, J., "An extended/generalized phase-field finite element method for crack growth with global-local enrichment", ***International Journal for Numerical Methods in Engineering***, Vol. 121, No. 11, (2020), 2534–2557. doi:10.1002/nme.6318
37. Okodi, A., Li, Y., Cheng, R., Kainat, M., Yoosef-Ghodsi, N., and Adeeb, S., "Crack Propagation and Burst Pressure of Pipeline with Restrained and Unrestrained Concentric Dent-Crack Defects Using Extended Finite Element Method", ***Applied Sciences***, Vol. 10, No. 21, (2020), 7554. doi:10.3390/app10217554
38. Moes, N., Dolbow, J., and Belytschko, T., "A finite element method for crack growth without remeshing", ***International Journal for Numerical Methods in Engineering***, Vol. 46, No. 1, (1999), 131–150. doi:10.1002/(SICI)1097-0207(19990910)46:1<131::AID-NME726>3.0.CO;2-J
39. ABAQUS User Manual, V. 6.12. Providence RI, USA: DS SIMULIA Corp, (2012).
40. REMMERS, J., DEBORST, R., and NEEDLEMAN, A., "The simulation of dynamic crack propagation using the cohesive segments method", ***Journal of the Mechanics and Physics of Solids***, Vol. 56, No. 1, (2008), 70–92. doi:10.1016/j.jmps.2007.08.003
41. Zeng, Q., and Yao, J., "Numerical Simulation of Fluid-Solid Coupling in Fractured Porous Media with Discrete Fracture Model and Extended Finite Element Method", ***Computation***, Vol. 3, No. 4, (2015), 541–557. doi:10.3390/computation3040541
42. Hansbo, A., and Hansbo, P., "A finite element method for the simulation of strong and weak discontinuities in solid mechanics", ***Computer Methods in Applied Mechanics and Engineering***, Vol. 193, Nos. 33–35, (2004), 3523–3540. doi:10.1016/j.cma.2003.12.041
43. Song, J.-H., Areias, P. M. A., and Belytschko, T., "A method for dynamic crack and shear band propagation with phantom nodes", ***International Journal for Numerical Methods in Engineering***, Vol. 67, No. 6, (2006), 868–893. doi:10.1002/nme.1652
44. Chen, Z., Liu, J., and Qiu, H., "Solidification Crack Evolution in High-Strength Steel Welding Using the Extended Finite Element Method", ***Materials***, Vol. 13, No. 2, (2020), 483. doi:10.3390/ma13020483
45. Moës, N., and Belytschko, T., "Extended finite element method for cohesive crack growth", ***Engineering Fracture Mechanics***, Vol. 69, No. 7, (2002), 813–833. doi:10.1016/S0013-7944(01)00128-X
46. Fallah, N., "A Development in the Finite Volume Method for the Crack Growth Analysis without Global Remeshing", ***International Journal of Engineering, Transaction A: Basics***, Vol. 29, No. 7, (2016), 898–908. doi:10.5829/idosi.ije.2016.29.07a.03
47. Sukumar, N., Moes, N., Moran, B., and Belytschko, T., "Extended finite element method for three-dimensional crack modelling", ***International Journal for Numerical Methods in Engineering***,

Vol. 48, No. 11, (2000), 1549–1570. doi:10.1002/1097-0207(20000820)48:11<1549::AID-NME955>3.0.CO;2-A

48. Gravouil, A., Moës, N., and Belytschko, T., "Non-planar 3D crack growth by the extended finite element and level sets-Part II: Level set update", ***International Journal for Numerical Methods in Engineering***, Vol. 53, No. 11, (2002), 2569–2586. doi:10.1002/nme.430
49. Duan, Q., Song, J.-H., Menouillard, T., and Belytschko, T., "Element-local level set method for three-dimensional dynamic crack growth", ***International Journal for Numerical Methods in Engineering***, Vol. 80, No. 12, (2009), 1520–1543. doi:10.1002/nme.2665
50. Nistor, I., Pantalé, O., and Caperaa, S., "Numerical implementation of the eXtended Finite Element Method for dynamic crack analysis", ***Advances in Engineering Software***, Vol. 39, No. 7, (2008), 573–587. doi:10.1016/j.advengsoft.2007.06.003
51. Motamedi, D., and Mohammadi, S., "Dynamic analysis of fixed cracks in composites by the extended finite element method", ***Engineering Fracture Mechanics***, Vol. 77, No. 17, (2010), 3373–3393. doi:10.1016/j.engfracmech.2010.08.011
52. Khademhosseini Beheshti, H., Haji Aboutalebi, F., and Najimi, M., "Stress Intensity Factor Determination in Functionally Graded Materials, Considering Continuously Varying of Material Properties", ***International Journal of Engineering, Transaction C: Aspects***, Vol. 29, No. 12, (2016), 1741–1746. doi:10.5829/idosi.ije.2016.29.12c.13
53. Rong, B., Rui, X., Tao, L., and Wang, G., "Theoretical modeling and numerical solution methods for flexible multibody system dynamics", ***Nonlinear Dynamics***, Vol. 98, No. 2, (2019), 1519–1553. doi:10.1007/s11071-019-05191-3
54. Sadripour, S., Estajloo, M., Hashemi, S., and Adibi, M., "Experimental and Numerical Investigation of Two Different Traditional Hand-Baking Flatbread Bakery Units in Kashan, Iran", ***International Journal of Engineering, Transaction B: Applications***, Vol. 31, No. 8, (2018), 1292–1301. doi:10.5829/ije.2018.31.08b.18
55. Gustafsson, A., Khayyeri, H., Wallin, M., and Isaksson, H., "An interface damage model that captures crack propagation at the microscale in cortical bone using XFEM", ***Journal of the Mechanical Behavior of Biomedical Materials***, Vol. 90, (2019), 556–565. doi:10.1016/j.jmbbm.2018.09.045

Persian Abstract

چکیده

رفتار سد قوس بتونی ترک خورده به دلیل شدت زمین لرزه و تغییر فشار آب مورد بررسی قرار گرفت. برای طراحی مدل‌های سد با مقاومت طراحی ۴۵ مگاپاسکال از بتن ساده استفاده شده است. یک جدول لرزش برای ایجاد یک مرکز آزمایش پویا برنامه‌ریزی، تولید و ساخته شده است. کار آزمایشی شامل آزمایش چهار مدل سد بتونی مقیاس‌پذیر بود که به دو گروه تقسیم شده است، هر گروه شامل دو درجه مختلف مدل انحنا است. یک شکاف مصنوعی در مرکز بدنه سد ایجاد شد. روش المان محدود توسعه یافته (XFEM) به منظور پرداختن به محمول عددی برای انتشار یک ترک، بیان شده است. نتایج نشان داد که رفتار خوب تمام سدهای قوسی تحت شدت متوسط زلزله وجود دارد. سد قوسی با درجه انحنای بالاتر به ترتیب ۱۷/۸ ٪ و ۱۶/۲ ٪ جابجایی کمتری را در جهت Z و X ثبت کرد. ارزیابی تنش و انتشار ترک در مقایسه با سد قوسی دارای کمترین درجه انحنا است. از این رو، افزایش درجه انحنا منجر به افزایش پایداری سد، مقاومت در برابر زلزله، جابجایی کمتر و رشد کمتر ترک‌های کششی شد.